

Analysis of a diode with a ferroelectric cathode

L. Schachter, J. D. Ivers, J. A. Nation, and G. S. Kerslick
*Laboratory of Plasma Studies and School of Electrical Engineering, Cornell University, Ithaca,
New York 14853*

(Received 21 August 1992; accepted for publication 25 February 1993)

It has been shown experimentally that electron current densities of more than 30 A/cm^2 can be achieved from a cathode made of ferroelectric ceramic, when applying a field of order 0.1 MV/m . This current exceeds the Child–Langmuir current by two orders of magnitude. The current in the diode varies linearly with the applied voltage, provided that the latter is positive. In this theoretical study we show that the ferroelectric material plays a crucial role in the emission process. When a voltage is applied to the ferroelectric, the internal polarization field varies and the amount of screening charge required decreases. As a result, the electrons distribution near the cathode changes, forming a cloud which fills part of the diode gap. If now a positive voltage is applied to the anode, electrons are readily transferred through the diode gap. The qualitative and quantitative results of the theory are in good accordance with the experiment.

I. INTRODUCTION

In the recent years a renewed interest in ferroelectric ceramics for generation of electron beams has been initiated by Riege and his collaborators at CERN.^{1–3} High intensity electron beams, 100 A/cm^2 , were produced for a pulse duration of $10\text{--}100 \mu\text{s}$ containing between 1 nC to several μC of charge. At the Lebedev Institute, Airapetov *et al.*⁴ measured current densities of 400 A/cm^2 in a diode of $0.3\text{--}1.0 \text{ mm}$ gap, with an extraction (gap) voltage of 1.6 kV at high repetition rate and with a total (train) pulse duration of 160 ns . We have examined the operation of a similar device^{5–9} but with a diode gap of $2\text{--}10 \text{ mm}$ width, extraction voltage lower than 250 V ($200\text{--}600 \text{ ns}$), and a 100-ns -long switching voltage. The maximum current density measured was 70 A/cm^2 , which is almost two orders of magnitude above the Child–Langmuir limit.

The basic mechanism is what we call externally controlled field emission, namely, the electrons extraction is due to an electric field which is generated *behind* the cathode and, at least in the regime our system was operated, it is almost unaffected by the anode voltage. General speaking the device consists of a ferroelectric slab which has a very nonlinear response to an applied voltage and if we were to determine a characteristic dielectric coefficient this would have been larger than several thousands. The slab has a uniform electrode on its back side and a gridded and grounded electrode on the front which faces the diode. This is the cathode. A uniform piece of carbon consists the anode. A voltage can be applied to the back electrode of the ferroelectric. If no such voltage is applied, the system behaves like a regular diode and practically for the anode voltage we are interested on, the current is zero. When the ferroelectric is pulsed, a substantial amount of current is measured.

A closer look to the system when a positive potential is applied to the back surface of the ferroelectric indicates its polarization state changes and the amount of charge required to screen the internal field varies according to the material characteristics. It cannot return the external

charge to the source but it can expel them into the gap. For this purpose the ferroelectric has to extract them from the metallic grid. At this point the geometry of the grid comes into play. The local electric field near each one of the grounded strips is sufficient to extract the electrons from the metal. The amount of charge repelled is determined by the electrical characteristics of the ferroelectric, the voltage applied on the back electrode, and the *electrostatic coupling* of the ferroelectric to the gap via the grid. In our experiment the anode voltage plays practically no role in this process. The electron cloud in the gap forms a “distributed cathode” which allows electrons to flow to the anode, if a voltage is applied on the latter.

The fact that the emission process is controlled by an external electric field which is not the one which accelerates the electrons in the diode, has the potential of producing high quality beams. For two other processes in which the emission is controlled externally the beam quality is limited by an increase in the temperature associated with the emission process. In the case of thermionic emission the cathode is heated such that the electrons in the metal acquire enough kinetic energy to locally overcome the work function and they form a cloud above the surface. Thus to heat the cathode is essential for emission. For photoemission the cathode is illuminated by a laser beam whose photons supply the energy required by the electrons to overcome the work function. However, today’s materials have low quantum efficiency.

In the present study we shall first review the experimental results (Sec. II) and then we shall give a detailed theoretical interpretation of the various processes which occur when pulsing a ferroelectric ceramic, Sec. III.

II. REVIEW OF EXPERIMENTAL RESULTS

A. Experimental setup

The experimental setup is shown schematically in Fig. 1. A 1-mm -thick, 2.5-cm -diam ferroelectric disk is coated with a thin uniform silver layer on the back and a gridded

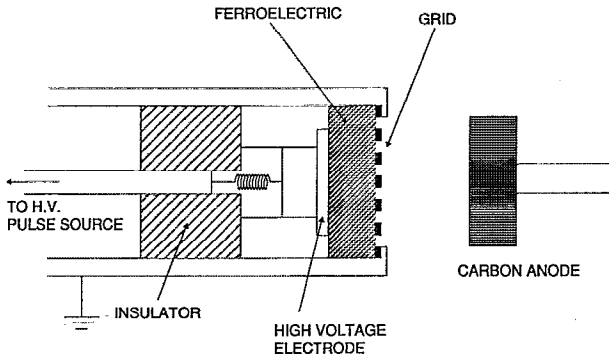
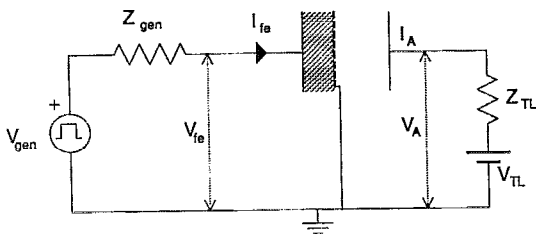


FIG. 1. The schematic experimental setup.

silver layer on its front surface; in both cases the thickness is $1\ \mu\text{m}$. The silver strips are $200\ \mu\text{m}$ wide and are separated by a similar distance. A metallic hat holds the ceramic tight and also provides the electric connection to the ground; the diameter of the hat is about $1\ \text{cm}$. The effective surface of emission is approximately $A \approx 0.8\ \text{cm}^2$. For these experiments we used lead zirconate titanate as the ferroelectric sample. This sample is mounted as a load on a $10\ \Omega$ transmission line which generates a $150\ \text{ns}$, $1\text{--}3\ \text{kV}$ pulse. A positive pulse is applied to the back electrode of the ferroelectric and the grid is grounded. The highly capacitive ferroelectric load is shunted by a $22\ \Omega$ resistor to improve the pulse shape. A planar carbon anode is located at a distance of $g \approx 1\text{--}10\ \text{mm}$ from the grid. The anode is maintained at a positive potential, V_{TL} , by a charged transmission line whose characteristic impedance can be varied between $R_{TL} = 12.5\ \Omega$ and $50\ \Omega$. The length of the anode voltage pulse is determined by the length of this line, which like the impedance, can be varied. A base pressure of 10^{-5} Torr is maintained in the diode.

Three quantities are directly measured: (1) the current charging the ferroelectric capacitor (I_{FE}), (2) the voltage across the ferroelectric (V_{FE}), and (3) the discharging current of the transmission line (the anode current I_{AN}). The upper frame in Fig. 2 illustrates typical anode current results for three shots corresponding to three different voltages ($V_{TL} \approx 100, 300,$ and $500\ \text{V}$) applied to a $25\ \Omega$ cable when the gap was $4\ \text{mm}$ wide. From a large number of such shots we have determined the $I\text{--}V$ of the diode. Figure 3 illustrates the diode characteristic curve as measured for several cables impedances and lengths. The current into the ferroelectric can be integrated to give the charge; the hysteresis curve describing the ferroelectric capacitor char-

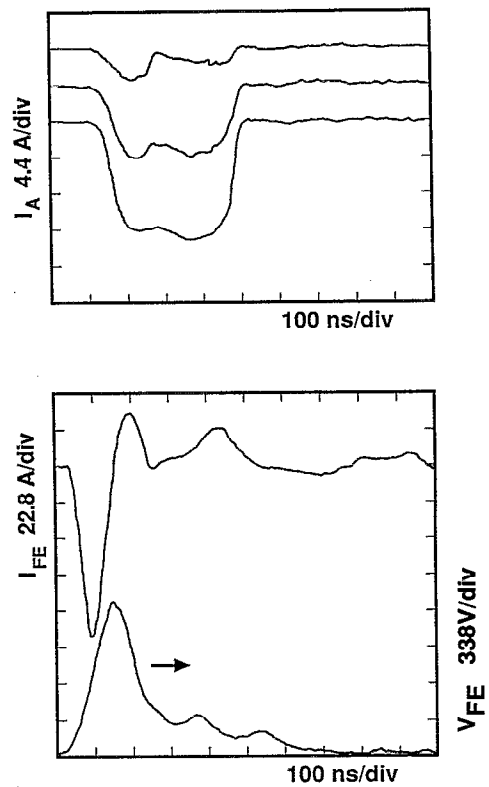


FIG. 2. One set of three shots corresponding to $V_{TL} = 100, 300,$ and $500\ \text{V}$ and a 4-mm -wide gap; $Z_{TL} = 25\ \Omega$ and the transmission line pulse is $400\ \text{ns}$ long. In the upper frame the anode currents are illustrated. In the lower frame the charging currents (I_{FE}) and the voltage on the ferroelectric (V_{FE}) are presented. All three shot are indistinguishable in this case. Notice that the voltage pulse on the ferroelectric is only about $150\ \text{ns}$ long.

acteristics during the (current) pulse shown in Fig. 2 is illustrated in Fig. 4. For comparison in Fig. 5 we present the schematics of the hysteresis curve measured at $60\ \text{Hz}$ and the electronic circuit used.

B. Main results

Next the experimental data accumulated are summarized. Most of the subjects are further considered in the

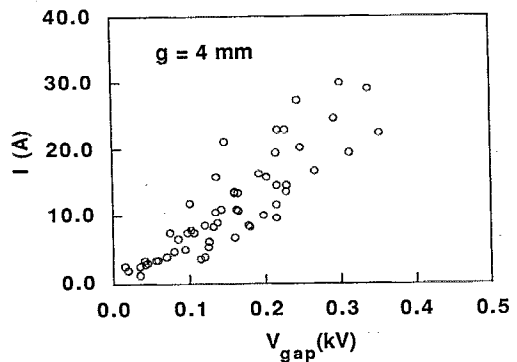


FIG. 3. The $I\text{--}V$ characteristic of a diode with a 4-mm -wide gap. Similar results were measured for $2, 6, 8,$ and $10\ \text{mm}$ gaps.

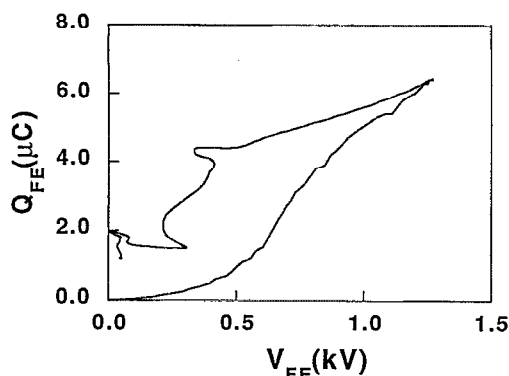


FIG. 4. The Q - V characteristic of the ferroelectric in the course of one shot.

theoretical section and we emphasize those which we consider to be of greater importance [(b) and (g)].

(a) In our regime of operation, the voltage on the ferroelectric is *not* affected by the current in the gap, see Fig. 2.

(b) The anode current continues even after the signal from the generator pulsing the ferroelectric is effectively off; its length is determined by the length of the cable as could be observed in Fig. 2. We shall explain this result in the next section.

(c) The shape of the anode current for low values ($I_A < 15$ A) is regular and, as illustrated in Fig. 2 (upper frame), it is relatively uniform; at higher levels the shape is rather triangular.

(d) At this stage of the experiments it appears that there is no significant difference in the operation of the device when the ferroelectric is pulsed with a positive or negative voltage.

(e) The Q - V curve of the ferroelectric capacitor for *slow* variations in the voltage and charge reveals a hysteresis characteristic. This curve may be approximately described by

$$D = \epsilon_0 \left[E + E_0 \tanh \left[(\epsilon - 1) \frac{E}{E_0} + \tanh^{-1} \left(\frac{P}{\epsilon_0 E_0} \right) \right] \right]. \quad (1)$$

Based on the hysteresis state of experimental data we determined the parameters of this curve to be $E_0 \approx 1.7 \times 10^{10}$ V/m, $\epsilon \approx 3000$, and $P_0 \approx 0.1$ C/m², where $P = \pm P_0$.

(f) Throughout our experiments I_{FE} is larger by at least one order of magnitude (≈ 100 A) than the anode current ($I_A \approx 0$ –25 A).

(g) The I - V curve of the gap appears to be *linear* (see Fig. 3) and for a given voltage, the current exceeds by two orders of magnitude the Child–Langmuir limit. If the diode gap is relatively narrow (< 10 mm), we found that the slope of this curve is strongly influenced by the voltage applied to the ferroelectric. One of the main goals in the next section is to determine the mechanism and find an adequate model to describe these effects.

(h) For narrow diode gap (< 2 mm) current was measured on the anode even for zero applied transmission line voltage. This current seems to be strongly dependent on the current charging the ferroelectric capacitor.

III. THEORY

For a complete description of the various processes in a diode with ferroelectric cathode, it is necessary to have an understanding of what happens: (1) in the ferroelectric, (2) at the grid surface, and (3) in the gap. In this section we suggest, for each one of these regions, a relatively simple model which, when all combined together, reveal a reasonable agreement with the experiment.

A. Overview

The ferroelectric material plays the key role in this device. If a voltage is applied on the gap, without pulsing the ferroelectric, the current measured (noise) is of order of tenth of amperes, whereas when the latter is pulsed currents of 15 A and more are monitored. Therefore it is crucial to understand the role of the ferroelectric. In order to avoid any misunderstanding we wish to point out that there is also overwhelming evidence that the currents mentioned above are not a result of a breakdown or ions effect since when large negative voltage is applied on the gap the current is practically zero.

When a positive voltage is applied on the back of the ferroelectric, electrons are brought to the metallic strips which consist the grid. The ferroelectric tends to maintain its initial state both at the global level (whole sample) and local level, i.e., near each metallic strip. Globally it cannot return the electrons to the source but locally, it can extract part of the new electrons from the strips and “place” them in the gap between the grid strips. In this way, the local change in the local density is minimized. The positive charge in the back of the ferroelectric attracts the electrons which are between the strips whereas the electrons which remained on the strips, repel them. The net result is that the “free” electrons are repelled into the gap where they form a cloud which is in *equilibrium* with the negative charge on the grid and the positive charge on the back

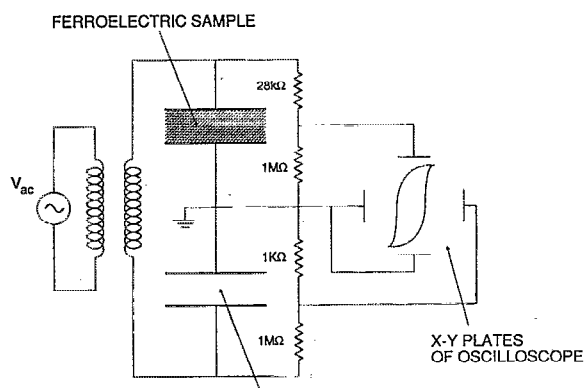


FIG. 5. The schematics of the hysteresis curve at 60 Hz and the circuit used for this measurement.

electrode. The actual extraction of the electrons from the surface is made possible by (i) the geometry of the grid, (ii) the electric field applied on the ferroelectric, and (iii) the internal electric (polarization) field of the material. The latter was shown in the previous section to exceed by many orders of magnitude the electric field necessary to extract electrons from a metal. In the gap those electrons are in a dynamic equilibrium, in the sense that they oscillate in a potential well induced by their own presence, the ferroelectric, and the grid, in other words, this well is a result of electrostatic coupling of these components. The net current associated with this motion is zero. As the voltage is applied on the anode, the motion is altered and a significant current is measured.

In the remainder of this section we shall consider the processes in the ferroelectric, the grid, and the gap separately. Each process is described by a relatively simple model. At the end we shall combine all the models together to simulate the operation of the device. In the next subsection we examine the behavior of the ferroelectric. In Sec. III C we analyze the electrical characteristics of the grid. This is followed by an analysis of the current flow in the gap when the electrons are inside. Finally in Sec. III E we determine the equations which describe the dynamics of the entire system; the equations are solved numerically.

B. The ferroelectric ceramic

We emphasized in the previous subsection that the important characteristics of the device are controlled by the ferroelectric material. In this subsection we shall examine¹⁰ the electrical properties of such a ceramic.

1. Bulk dynamics

Consider a material whose molecular or atomic structure is characterized by the microscopic dipole moment, which in a 1D model, is denoted by p . The effective electric field E_{eff} , which affects each individual dipole, has two components: one is due to the external electric field E and the second represents the electric field generated in the material by all the other dipoles, hence

$$E_{\text{eff}} = E + P \frac{1}{\epsilon_1}. \quad (2)$$

This field is called the polarization field P ; $\epsilon_1 = \epsilon_0 \epsilon_r$, where $\epsilon_0 = 8.85 \times 10^{-12}$ F/m, and ϵ_r is a characteristic of the material. We denote by N_+ and N_- the number of dipoles per unit volume with positive or negative polarity, respectively. Using this notation, the polarization field P is defined as

$$P \equiv p(N_+ - N_-). \quad (3)$$

We shall next assume, for the moment, that variation in the polarization field is due to change in the number of dipoles per unit volume rather than variation of an individual dipole, thus

$$\frac{dP}{dt} = p \left(\frac{dN_+}{dt} - \frac{dN_-}{dt} \right). \quad (4)$$

The transition rate of a dipole from positive to negative polarity is denoted by T_{+-} . In a similar way T_{-+} repre-

sents the transition probability the other way around; positive and negative refer here to the alignment of the dipole relative to the effective electric field present in its vicinity. Within the framework of a linearized transition theory we can determine the following dynamics for the dipoles:

$$\begin{aligned} \frac{dN_+}{dt} &= T_{-+}N_- - T_{+-}N_+, \\ \frac{dN_-}{dt} &= T_{+-}N_+ - T_{-+}N_-. \end{aligned} \quad (5)$$

The transition rate is determined by the deviation from equilibrium generated by the effective electric field which acts on the individual dipole, i.e.,

$$\begin{aligned} T_{+-} &= \Omega e^{pE_{\text{eff}}/k_B T}, \\ T_{-+} &= \Omega e^{-pE_{\text{eff}}/k_B T}, \end{aligned} \quad (6)$$

where k_B is Boltzmann's constant, T is the equilibrium temperature, and Ω is a characteristic of the material. The total number of dipoles per unit volume, N , is assumed to be known

$$N_+ + N_- = N. \quad (7)$$

Thus we substitute Eqs. (3), (5)–(7) in Eq. (4) and find that

$$\begin{aligned} \frac{dP}{dt} + 2\Omega P \cosh\left(\frac{p(E+P/\epsilon_1)}{k_B T}\right) \\ = 2pN\Omega \sinh\left(\frac{p(E+P/\epsilon_1)}{k_B T}\right). \end{aligned} \quad (8)$$

This is the equation which determines the dynamics of the polarization field in the material. It is convenient to define $P_1 = pN$, $\tau = 1/2\Omega$, $\theta = t/\tau$, $E_1 = k_B T/p$, $\psi = P_1/\epsilon_1 E_1$, $\bar{V} \equiv E/E_1$, and $\bar{P} \equiv P/P_1$; using this notation we can write Eq. (8) as

$$\frac{d\bar{P}}{d\theta} + \bar{P} \cosh(\bar{V} + \psi\bar{P}) = \sinh(\bar{V} + \psi\bar{P}). \quad (9)$$

2. Finite size effects

One of the immediate features of the expression in Eq. (9) is the spontaneous polarization which may occur below a given (Curie) temperature. In equilibrium, $d\bar{P}/d\theta = 0$, and when no external field is applied ($\bar{V} = 0$), Eq. (9) reads

$$\bar{P} = \tanh(\psi\bar{P}). \quad (10)$$

In Fig. 6 we illustrate the numerical solution of this equation. We observe that a solution is possible only if $\psi > 1$ ($\psi = 1$ determines the Curie temperature). Although only the positive solution is presented in the figure, from the symmetry of Eq. (10) we conclude that the negative solution behaves similarly.

Let us now consider a thin slab of ferroelectric (radius R and thickness d). As a starting point let us assume that the material was prepared in ideal vacuum such that the ferroelectric is the only material in the experiment and no

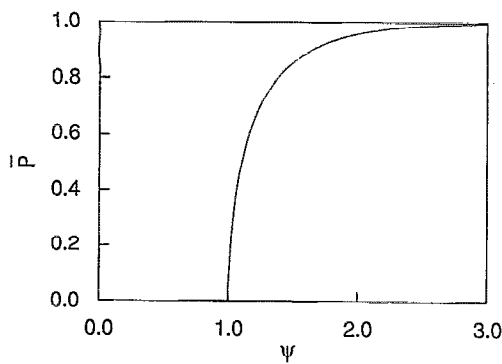


FIG. 6. Spontaneous normalized polarization field \bar{P} as a function of the parameter ψ . For $\psi < 1$ the spontaneous polarization is zero.

other atoms (ions or electrons) are available. In these circumstances we ask what is the electric field which would be measured out of the material? For the simplicity we shall assume that the polarization field is uniform and it is directed in the z direction (which also coincide with the disk axis). To answer this question we must solve the Poisson equation:

$$\phi(r, z) = -\frac{1}{4\pi\epsilon_0} \int dV' \nabla' \mathbf{P} \frac{1}{|\mathbf{r} - \mathbf{r}'|}. \quad (11)$$

Here we used the usual definition of $\mathbf{D} = \epsilon_0 \mathbf{E} + \mathbf{P}$. Since the polarization field is assumed to be uniform then $\nabla' \mathbf{P} = 0$ except at $z = -d$ and $z = 0$. This implies that in these conditions, the polarization field acts as if two disks of free charge were present at these two planes; the effective charge distribution reads

$$\rho_{\text{eff}} = P[-\delta(z+d) + \delta(z)]. \quad (12)$$

Out of the material \mathbf{D} and \mathbf{E} are parallel since $\mathbf{D} = \epsilon_0 \mathbf{E}$. The boundary conditions at $r = R$ imply that the electric field in the material is negative, though the electric induction \mathbf{D} is still positive. For simplicity let us further assume that the electric field is uniform in the slab (practically this is equivalent to considering its average value).

In this simple minded model the polarization field is the only source of the electrostatic energy, therefore by virtue of the linearity of the Poisson equation we may conclude that $\mathbf{E} = -\chi \mathbf{P}$, where χ is a positive constant which depends entirely on the geometry of the slab. Using the notation prior to Eq. (9), the equilibrium polarization state is a solution of

$$\bar{P} = \tanh(\bar{V} + \psi \bar{P}) = \tanh(-\chi \bar{P} + \psi \bar{P}). \quad (13)$$

We conclude therefore that the finite size of the sample tends to reduce the polarization of the material.

In spite the finite geometry effect, a significant electric field is still available (recall that in the previous section $E_0 \approx 10$ GV/m). Therefore if we now release the constraint of ideal vacuum, we find that the field generated by the ceramic strongly attracts any charge from the surroundings. In practice, the effective free charge distribution which represents the ferroelectric in ideal vacuum is com-

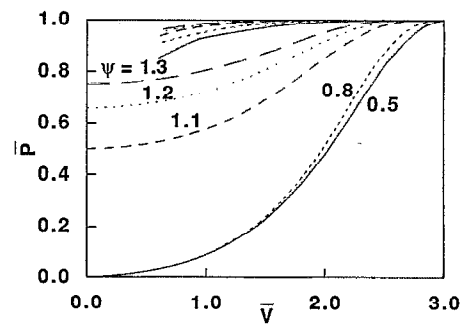


FIG. 7. The variation of the normalized polarization field as a function of the voltage for various values of the parameter ψ . If the initial polarization is zero and a positive voltage is applied, the change in the polarization field is much smaller than if the ceramic is initially nonpolarized.

pletely canceled in a practical vacuum system. In other words (again assuming positive P), a layer of holes from the surroundings will cancel the effective electron layer at $z = -d$ [see Eq. (12)] and a layer of electrons will screen the positive charge at $z = 0$. Since the effective free charge is now zero, the electric field out of the material is zero. As in the previous case, we examine the boundary conditions at $r = R$ and conclude that the electric field in the ceramic must be zero ($E_{\text{internal}} = 0$). Now it is possible to examine the same problem reversing the arguments, namely, we know experimentally that no voltage is measured on the ferroelectric, therefore the internal electric field must be identically zero. If this is the case, then $\mathbf{D} = \mathbf{P}$, and on the front surface we may expect a free charge

$$Q_{\text{front}} = -DA = -PA, \quad (14)$$

whereas on the back counterpart

$$Q_{\text{back}} = DA = PA, \quad (15)$$

where $A = \pi R^2$ is the surface of the electrode. It is interesting to note that the total electrostatic energy stored in the system is zero whereas in the former case (ideal vacuum) the energy was nonzero, therefore we may expect that any system which consists of ferroelectric ceramic tends to reach this minimum energy state.

3. Dynamic processes

In the present experiment, the voltage applied on the ferroelectric capacitor is varying in time. Let us now consider the polarization of the ferroelectric for two different pulses. First, we shall examine the case when $\bar{V} = 3\theta e^{-\theta+1}$. The normalized polarization field as calculated from Eq. (9) is illustrated in Fig. 7 for various values of ψ . The two curves which start from zero correspond to values of ψ below unity. All five curves are in good qualitative agreement with the experimental curve in Fig. 4. From these curves we conclude that when a positive voltage is applied, the polarization change is much larger if the material is not initially polarized comparing to the case when some initial polarization exists. It is interesting to note that the polarization remains high even after the pulse has decayed to zero, as illustrated in Fig. 8. Later it will be shown that this

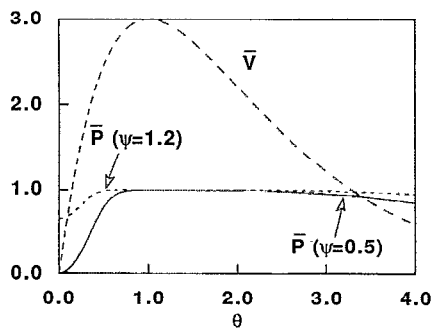


FIG. 8. The variation of the normalized polarization field and the applied voltage in time. The polarization remains high even after the pulse has practically decayed to zero.

effect is directly responsible to the fact that the length of the current pulse in the diode is controlled by the anode voltage rather than the pulse on the ferroelectric.

The other case of interest is when a periodic pulse is applied to such a capacitor. Except during a relatively short transient, the polarization field follows a well-defined hysteresis curve as illustrated in Figs. 9, 10, and 11. In the first case $\psi=0.9$, therefore the starting point is zero; in the second and third $\psi=1.1$. In the first two cases the pulse is $\bar{V}=7 \sin(4\pi\theta)$ with $\theta < 2$. In the third $\bar{V}=-7 \sin(4\pi\theta)$ and we observe that maximum change in the polarization is expected when actually the polarization is reversed. In all three cases the hysteresis curve is completed three times. From the examples above we see in a systematic way what we indicated previously in a rather intuitive fashion, namely, that there should be a significant difference in the response of the material if it is positively polarized and a positive or negative voltage is applied. On the other hand, if the system is not initially polarized (the case $\psi < 1$) the response is symmetric.

4. The ferroelectric capacitor

Together with its two electrodes, the ferroelectric sample constitutes a nonlinear capacitor. We now determine the Q - V relation of this capacitor based on the dynamics of the material [Eq. (9)]. In Eq. (15) we have determined the amount of free charge present on the back of the capacitor

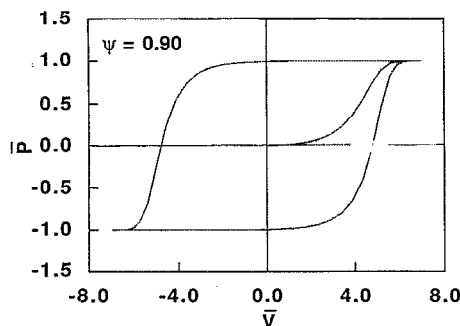


FIG. 9. The hysteresis curve for a periodic voltage starting from zero initial conditions, i.e., $\psi=0.9$. The normalized voltage is $\bar{V}=7 \sin(4\pi\theta)$.

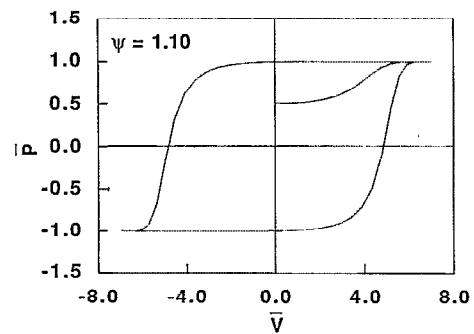


FIG. 10. The hysteresis curve for a periodic voltage starting from non-zero initial conditions, i.e., $\psi=1.1$. The normalized voltage is $\bar{V}=7 \sin(4\pi\theta)$.

when no external voltage is applied. It has also been shown that the polarization field acts as if a layer of free charge was present on both electrodes. In this way, the total amount of free charge on each electrode is zero. When a voltage is applied, the amount of free charge is varied but in the same time the polarization field changes and consequently, the amount of free charge required to screen this field varies. Let us denote by Q_p the amount of charge which represents the polarization field on the back electrode of the ferroelectric. Based on Eq. (15) we can actually define $Q_p \equiv PA$. In the presence of an external field this charge varies according to

$$\begin{aligned} \frac{dQ_p}{dt} + 2\Omega Q_p \cosh\left(\frac{V_{FE} + Q_p/C_p}{V_1}\right) \\ = 2\Omega Q_0 \sinh\left(\frac{V_{FE} + Q_p/C_p}{V_1}\right), \end{aligned} \quad (16)$$

where V_{FE} is the voltage on the capacitor, $V_1 = k_B T d / p$, $C_p = \epsilon_1 A / d$, and $Q_0 = P_1 A$. The equilibrium (real) free charge there is denoted by $Q^{(eq)}$ and it is a solution of

$$Q^{(eq)} = Q_0 \tanh\left(\frac{Q^{(eq)}}{C_p V_1}\right). \quad (17)$$

The free charge due to the applied voltage is denoted by Q_{app} and is given by $C_0 V_{FE}$ where $C_0 = \epsilon_0 A / d$. The total

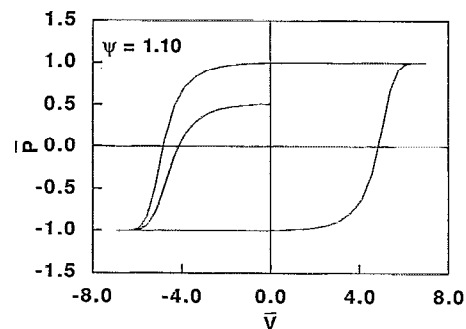


FIG. 11. The hysteresis curve for a periodic voltage starting from zero initial conditions, i.e., $\psi=1.1$. The normalized voltage is reversed $\bar{V}=-7 \sin(4\pi\theta)$.

change in the charge, Q_{FE} , of the capacitor is $Q_{FE} \equiv Q_p + Q_{app} - Q^{(eq)}$. Accordingly the current in the ferroelectric capacitor is

$$I_{FE} \equiv \frac{dQ_{FE}}{dt} = \frac{dQ_p}{dt} + C_0 \frac{dV_{FE}}{dt}, \quad (18)$$

where Q_p is self-consistent solution of Eq. (16). The connection between the two sets of parameters, in Eqs. (17) and (1), is discussed in Appendix A.

We assumed in the previous subsection that p , the dipole moment of the material, is constant. If we closely examine Fig. 4, we observe that the saturation level reached by the ferroelectric appears to vary with the voltage. The model which describes the ferroelectric capacitor can be further generalized if the constraint of constant p is released. Based on the experimental data in Fig. 4 we found very good evidence that the dipole moment of the material is linearly dependent on the applied voltage. Using the present notation this can be formulated as

$$Q_0 = Q_{00} + C_{eff} V_{FE}, \quad (19)$$

where $C_{eff} \equiv \epsilon_0 \epsilon_{eff} A/d$ and ϵ_{eff} is a parameter of the material which remains to be determined experimentally.

5. "Free" electrons

So far we have tacitly assumed that the front electrode of the capacitor is uniform. In the experiment, this electrode is gridded and it facilitates electron extraction. Let us ignore for the moment the capacitance associated with the grid geometry such that the charge variation in time can be directly concluded from the drawings of the polarization field in Figs. 7–11. In these figures we plotted the absolute value of the polarization and in the context of electrons extraction we have to consider the charge variation therefore one has to extract the value at $t=0$. For a given applied (positive) voltage, the largest amount of charge is available when the initial polarization is negative, i.e., when the polarization of the material is reversed by the applied voltage. A smaller amount is available when the material is not initially polarized and the least charge is present when the initial polarization is positive.

In Sec. III A we have described qualitatively the process which facilitates the extraction of electrons from the surface. The details of this process are beyond the scope of the present study and the fraction of electrons which are actually in the gap is left as a parameter of the model.

The conclusions from this subsection are (i) electrons are being repelled into the gap, (ii) the number of electrons in the gap depends on the initial polarization state and the applied voltage, (iii) electrons will be present in the gap as long as the polarization state of the ferroelectric is off equilibrium.

C. The grid: electrostatic considerations

The ceramic can affect the gap only because the interface electrode is gridded, otherwise no coupling would occur between the two regions. The metallic strips are grounded but in between the potential is nonzero. Conse-

quently the average potential on this electrode is nonzero. It can affect significantly the diode gap when the anode voltage is relatively low, but it does not seem to have a significant influence on the ferroelectric capacitor. In this study the electrical role of the grid is represented by its own capacitance.

In order to determine its capacitance we ignore the nonlinear behavior of the ferroelectric and solve an electrostatic problem using a linear dielectric coefficient, ϵ_{FE} instead. (In the last subsection this constraint is released and ϵ_{FE} is calculated at any instant according to the values of D and E in the ferroelectric.) The system is assumed to be uniform in the y direction ($\partial/\partial y=0$) and periodic in the x direction; the gridded electrode is located at $z=0$. Two uniform metallic plates located at $z=g$ and $z=-d$ represent the anode and the back electrode of the ferroelectric correspondingly; these two plates are assumed to be grounded. On each strip of the grid we assume a uniform charge distribution

$$\eta = \frac{Q_{strip}}{\Delta y(L-a)}, \quad (20)$$

where L is the periodicity and a is the strips separation; Δy represents a unit length in the y direction. This charge distribution can be readily represented as a Fourier series

$$\eta = \sum_{n=-\infty}^{\infty} \eta_n e^{-jk_n x}, \quad (21)$$

where $k_n \equiv 2\pi n/L$,

$$\eta_n = \frac{Q_{strip}}{\Delta y L} e^{jk_n(L+a)/2} \text{sinc}[k_n(L-a)/2], \quad (22)$$

and $\text{sinc}(\xi) \equiv \sin(\xi)/\xi$. Assuming that $d, g \gg L$, then the potentials are given by

$$\phi(x, z < 0) = \sum_{n \neq 0} \phi_{1,n} e^{-jk_n x} e^{-|k_n|z} \quad (23)$$

and

$$\phi(x, z > 0) = \sum_{n \neq 0} \phi_{2,n} e^{-jk_n x} e^{-|k_n|z}. \quad (24)$$

Imposing the boundary condition we find for $n \neq 0$ that

$$\phi_{1,n} = \phi_{2,n} = \eta_n \frac{1}{\epsilon_0(1 + \epsilon_{FE}) |k_n|}. \quad (25)$$

In a similar way for the zero harmonic we have $\phi_{1,0} = A_1 z + B_1$ and $\phi_{2,0} = A_2 z + B_2$; the four coefficients are

$$A_1 = -A_2 g/d, \quad B_1 = B_2 = -gA_2, \quad (26)$$

$$A_2 = \frac{\eta_0}{\epsilon_0(\epsilon_{FE} g/d + 1)}.$$

Finally we can calculate the entire electrostatic energy W_E stored in our system (in a unit surface $\Delta y L$). The capacitance of the system is

$$\frac{1}{C_{tot}} \equiv \frac{2W_E}{Q_{strip}^2} = \frac{1}{C_{grid}} + \frac{1}{C_{FE} + C_{gap}}, \quad (27)$$

where $C_{FE} = \epsilon_0 \epsilon_{FE} \Delta y L / d$ is the ferroelectric capacitance on this surface, $C_{gap} = \epsilon_0 \Delta y L / g$ is the gap capacitance, and finally for $a = L/2$ the grid capacitance is

$$C_{grid} = \epsilon_0 \Delta y L \left(0.5 (\epsilon_{FE} + 1) \frac{\pi^3}{1.2L} \right). \quad (28)$$

In our case $\epsilon_{FE} \gg 1$ and typically the separation of the electrodes from the grid (g and d) can be considered much larger than the grid periodicity L . Therefore from Eq. (28) we can readily deduce that since $C_{grid} \gg C_{FE} \gg C_{gap}$, the ferroelectric capacitance is dominant:

$$C_{tot} \approx C_{FE}. \quad (29)$$

The equivalent circuit which describes the generator and the ferroelectric operation, as one can conclude from the expression in Eq. (27), neglecting the gap capacitance, is two capacitors in series. The ratio between the grid and the ferroelectric capacitances determines the voltage on the grid in terms of the generator voltage in static conditions, i.e.,

$$V_{grid} \approx \frac{C_{FE}}{C_{grid}} V_{gen}. \quad (30)$$

It is beyond the scope of this study to investigate the details of the emission process from the cathode. However, some of the basic features of this process can be deduced from this simplified model. If we ignore the anode and consider the potential distribution near the cathode (in the gap side) we can approximate it with

$$\phi(z=0^+, x) \approx V_{grid} + V_{grid} \cos\left(\frac{2\pi x}{L}\right) e^{-2\pi z/L}. \quad (31)$$

The electric field near the metallic surface is therefore approximately $2\pi V_{grid}/L$. According to the parameters of our system and the relation in Eq. (30), $V_{grid} \approx 0.03 V_{gen}$. Therefore, a 1400 V applied on the back of the ferroelectric translates into 10^6 V/m near the metallic strips which face the diode gap. This electric field is not sufficient to extract electrons from the metal. However, near the edge of each strip the electric field is expected to be about 400 times larger (this is the ratio between the periodicity of the grid and the thickness of the silver strip). This value is more than sufficient for electrons' extraction from a metal. In addition, we did not consider here the process of extraction due to the electric field *induced* by the change in the polarization field. In fact we have reasons to believe that this is the dominant factor in the extraction process. There is some preliminary evidence regarding the grid's role as an electron source in narrow gap (< 2 mm) experiments. The current measured for $V_{TL} = 0$ indicates that the grid acts as a source of 40–60 V, which is in reasonable agreement with what one would calculate using Eq. (30).

D. The electron cloud

The direct result of the voltage applied on the ferroelectric is the change in the polarization field accompanied by electrons being repelled into the gap. The details of their distribution are calculated in Appendix B. According to

this calculation, the cloud may expand into the gap following a $\exp(-\epsilon_{FE} z/d)$ law; where ϵ_{FE} is the effective dielectric coefficient of the ferroelectric and d is the sample thickness.

1. The potential well—1D approximation

We do not have to know the details of the exact distribution of the electrons in order to estimate their impact on the the potential distribution in the gap. For this purpose we assume that (i) the plane of zero potential is actually on the cathode. From the fact that practically no current was measured for zero anode voltage ($g > 2$ mm) we deduce that (ii) the electric field near the anode behaves as if no electrons were injected into the gap. This can be understood since the cloud and the grid electrons form all together a "distributed cathode" which neutralizes the positive charge on the back of the ferroelectric; in other words, we do not expect the anode to be affected by the ferroelectric capacitor. Bearing in mind that (iii) the anode potential V_{AN} is known we consider a solution of the 1D Poisson equation which satisfies the three boundary conditions mentioned above:

$$\phi(z) = V_{AN} \frac{z}{g} + \Phi \frac{z(g-z)^2}{g^2}. \quad (32)$$

The unknown amplitude Φ is determined by substituting Eq. (32) in the Poisson equation and integrating the resulting expression over the entire length of the diode. The source term in the Poisson equation is then proportional to the charge in the gap and therefore so is Φ ; explicitly $\Phi = g |Q_{gap}| / 3\epsilon_0 A$, where A is the diode surface. From this simplified potential distribution we conclude that the potential has a maximum at $z = g/3$ and its value there is $\phi_{max} \approx \Phi/7$. If all the charge which initially was on the surface of the ferroelectric is repelled into the gap, ϕ_{max} is about four orders of magnitude larger than the typical anode voltage. Now we are in position to qualitatively understand the two order of magnitude increase in the anode current (comparing to Child–Langmuir limit). If instead of the usual $V_{AN}^{3/2}$ law we consider the case when the current is proportional to $\phi_{max}^{1/2} V_{AN}$, then clearly we find that the potential associated with the presence of the cloud is responsible to the two orders of magnitude increase in the current.

From the potential in Eq. (32) we deduce that the electrons in the cloud are in a dynamic equilibrium in which they oscillate in the potential well which is induced by their own presence, the ferroelectric and the boundary conditions, in the gap.

2. Gap resistivity

We have examined the influence of a strong magnetic field on the current flow in the diode and although the current shape was somewhat altered, the basic amount of current was unchanged. This indicates that the transverse motion of the electrons does not play a crucial role in this system. Therefore a one-dimensional model should be adequate to determine the dynamics of the electrons. We start

from the equilibrium state ($V_{AN}=0$). Due to the oscillatory character of the motion, the average velocity of the electrons is zero. However, this is because half of the electrons are moving to the anode whereas the other half toward the cathode. At any point these two flows are equal. We may estimate the average kinetic energy, $mc^2(\gamma_0-1)$, of the electrons by averaging the expression for the energy conservation over the gap spacing. Using Eq. (32) we found that γ_0 reads

$$\gamma_0 = 1 + \frac{1}{36} \bar{Q}, \quad \bar{Q} \equiv \frac{eQ_{\text{gap}}g}{\epsilon_0 A m c^2}. \quad (33)$$

As we may have expected, the average kinetic energy of the electrons increases linearly with the total amount of charge in the gap (Q_{gap}). To complete the description of the equilibrium state, we denote the average particle density in the cloud with \bar{n} and the lowest estimate of this quantity is just the total number of particles divided by the effective gap volume, i.e., $\bar{n} \approx Q_{\text{gap}}/egA$.

When a positive anode voltage V_{AN} is applied, the potential in the gap is $\phi_{\text{app}} = V_{AN}z/g$ since typically (in the conditions of our experiment) this potential is much smaller than the potential Φ associated with the gap charge and the charge density does not change. As in equilibrium, we can now calculate the average change in the velocity field of the two flows we mentioned above. Using again energy conservation we find

$$\delta\beta_+ = \frac{1}{\beta_0\gamma_0^3} \frac{1}{2} \frac{e}{mc^2} V_{AN}$$

and

$$\delta\beta_- = -\frac{1}{\beta_0\gamma_0^3} \frac{1}{2} \frac{e}{mc^2} V_{AN}, \quad (34)$$

corresponding to the outgoing and backflowing electrons. The total current in the system is determined by these two quantities and the charge density (which as previously mentioned is assumed to remain unchanged):

$$I_{AN} = eA\bar{n}c(\delta\beta_+ - \delta\beta_-). \quad (35)$$

This finally allows us to determine the gap resistance R_{gap} :

$$R_{\text{gap}} \equiv \frac{V_{AN}}{I_{AN}} = \eta \frac{1}{36} \frac{g^2}{A} \gamma_0^2 \sqrt{(\gamma_0+1)/(\gamma_0-1)}. \quad (36)$$

Where A is the diode surface and $\eta = 377 \Omega$. This is the main analytical result of this study, since it quantitatively shows that the presence of an electron cloud in the gap is directly responsible to the linear I - V characteristic measured experimentally. One can easily see that R_{gap} has a minimum as a function of γ_0 . This minimum occurs at $\gamma_0 = 1.28$ and for $g = 4 \text{ mm}$ and $R = 5 \text{ mm}$ it corresponds to $Q_{\text{gap}}^{\text{opt}} = 0.9 \mu\text{C}$ and $R_{\text{gap}}^{\text{min}} \approx 10 \Omega$, which agrees well with the experimental data.

The linear behavior of the I - V curve in the gap as demonstrated experimentally in Figs. 2 and 3 is represented theoretically by Eq. (36). This "Ohmic" behavior raises the question of the dissipation mechanism. To answer

this question one should recall that if we have a capacitor in which the capacitance itself may vary in time, then the current has two contributions:

$$I_{AN} = C_{\text{gap}} \frac{dV_{AN}}{dt} + V_{AN} \frac{dC_{\text{gap}}}{dt} \approx V_{AN} \frac{dC_{\text{gap}}}{dt}. \quad (37)$$

One contribution is from variation of the voltage in time whereas the second is from variation of the capacitance. The gap capacitance is small but change in the capacitance induced by the ferroelectric by injecting the electrons is large. Therefore the displacement contribution can be neglected. This expression indicates that the variation in the capacitance of the gap, resulting from the change in the capacitance of the ferroelectric capacitor, may be interpreted as an effective resistance: $dC_{\text{gap}}/dt = 1/R_{\text{gap}}$. Therefore the dissipation mechanism is effectively a result of the variation in time of the electrostatic energy stored in the ferroelectric as electrons are repelled into the gap. This is also the electrostatic (capacitive) coupling we were mentioning earlier.

The capacitive coupling between the ferroelectric capacitor and the diode gap is also the explanation to the difficulty raised by the minimal value of R_{gap} : the 10Ω value implies $\gamma_0 \approx 1.28$, which corresponds to a potential of 143 kV . And the question is what is the source of this voltage if the maximum voltage applied here was on the order of 2 kV on the ferroelectric? There are at least two ways to explain this phenomenon. (i) Imagine a capacitor (two metallic plates) with a dielectric slab [$\epsilon = 3000$ see Eq. (1) and the parameters thereafter] charged at 2 kV . If the dielectric is pulled out mechanically, the charge remains the same (since in this gedanken experiment the plates are not connected to the external world), thus the voltage will increase to 6 MV . In the real experiment, we have instead the dielectric a ferroelectric which as indicated in the previous subsections is a nonlinear medium. As voltage is applied, the effective dielectric coefficient is lowered (equivalent to pulling out the dielectric in the gedanken experiment), therefore the system tends to either get rid of electrons or increase the voltage. The voltage is set by the external source. The ferroelectric cannot reject these electrons to ground because the system is neutral and for each electron on the front electrode there is a "hole" on the back. Therefore the system repels electrons in the gap and the increased potential (due to capacitance variation) is induced into the gap as manifested by the presence of the electrons there. The 6 MV is obviously an overestimate of the possible voltage variation in the process which in addition to the fact that not all the electrons are actually repelled in the gap indicate that the 143 kV estimated above, are only a small fraction of the potential variation in the system. (ii) The other (equivalent) way to understand the source of these 143 kV which develop in the gap is to examine more closely what happens near the grid. According to the phenomenological parameters which describe the ferroelectric in Eq. (1), the characteristic electric field in the material is 17 GV/m . The electrostatic coupling between the ferroelectric slab and the diode gap is determined by the geometry of the grid. In particular this cou-

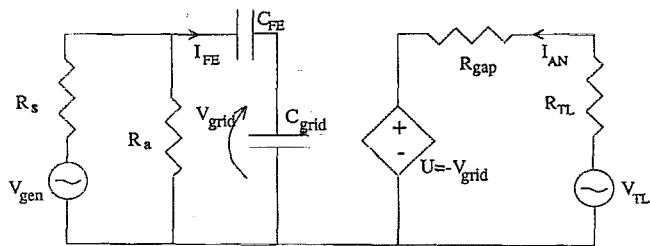


FIG. 12. The equivalent circuit of the system.

pling is represented by the distance between two adjacent strips, which is of the order of $200 \mu\text{m}$. Thus we can roughly estimate the maximum induced potential as the product of the two: $\Phi_{\text{ind,max}} \approx 17 \text{ GV/m} \times 200 \mu\text{m} = 3.4 \text{ MV}$. Like in the previous case this potential is by one order of magnitude larger than anticipated from the expression in Eq. (36). In order to understand the discrepancy we have to remember that the expression in Eq. (36) relies on averaging out the distribution of the electron cloud in the gap and the bottom point of the potential well is at $1/3$ of the gap. We know that this is not accurate (see Appendix B) and the more localized the distribution, the deeper the potential well. We wish to conclude this subsection with a comment: electrons which oscillate in this kind of potential well, radiate. Visible light was observed and we do not rule out the possibility of x rays being emitted. No quantitative attempts to measure this radiation have been made by us.

E. The dynamics of the system

At this point we are in position to review our main results and combine them in order to simulate the operation of the entire system. It was shown in Sec. III B 5 that the ferroelectric behaves like a nonlinear capacitor which is described by Eqs. (17)–(19). The grid's capacitance was calculated and an explicit analytic expression [Eq. (28)] was given in terms of the temporary (and effective) dielectric coefficient of the ferroelectric material. Finally, the anode cathode gap can be described by the gap impedance whose analytic expression [Eq. (36)] was brought in the last subsection. Based on the models mentioned above we have constructed an equivalent circuit which is illustrated in Fig. 12. There are three features in this system we wish to reemphasize: (i) the nonlinear character of the ferroelectric capacitor, (ii) the coupling between the two sections of the circuit is through the grid which allows (iii) the gap resistance to be determined by the amount of charge in the gap which in turn is a fraction the charge on the ferroelectric capacitor. The exact value of this fraction is determined by the detailed emission process and this is beyond the scope of the present study and we shall leave it as a parameter of the problem, i.e., $Q_{\text{gap}} = \nu Q_{\text{FE}} < Q_{\text{FE}}$. These are the equations which describe the system:

$$V_{\text{gen}} = I_s(R_s + R_a) - I_{\text{FE}}R_a, \quad (38)$$

$$(I_s - I_{\text{FE}})R_a = V_{\text{FE}} + V_{\text{grid}}, \quad (39)$$

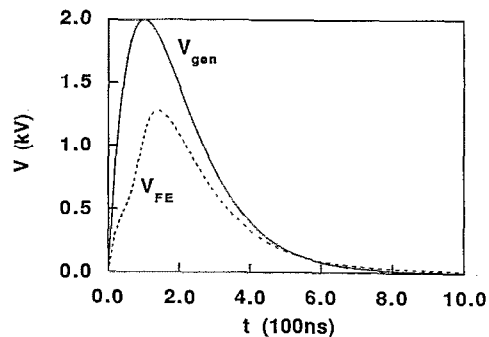


FIG. 13. The voltage on the ferroelectric V_{FE} as a function of time. As reference, the generator voltage is also plotted.

$$V_{\text{TL}} = I_{\text{AN}}(R_{\text{TL}} + R_{\text{gap}}) - V_{\text{grid}}, \quad (40)$$

in addition the grid capacitor determines $I_{\text{grid}} = (d/dt)C_{\text{grid}}V_{\text{grid}}$ and the relation between the voltage and the current on the ferroelectric capacitor is given in Eqs. (17)–(19). This system of equations has been solved numerically. During the simulation process it was found that the effect of the anode current on the grid voltage is minor and therefore we have ignored this process. The parameters in the following examples are $\Omega = 11 \times 10^6 \text{ rad/s}$, $V_1 = 800 \text{ V}$, $\epsilon_r = 7200$, $d = 1 \text{ mm}$, $g = 4 \text{ mm}$, $A = 0.785 \text{ cm}^2$, $L = 0.4 \text{ mm}$, $R_{\text{TL}} = 25 \Omega$. The two parameters in Eq. (19) are $Q_{00} = 4.0 \mu\text{C}$ and $\epsilon_{\text{eff}} = 3300$. The latter is determined from the slope of the upper hysteresis curve in Fig. 4.

At the first stage we consider only the ferroelectrics circuit, assuming that the electrode facing the gap is uniform. The generator pulse is given by $V_{\text{gen}}(\text{kV}) = 2.0\tau \exp(-\tau + 1)$, where $\tau = t/100 \text{ ns}$; this voltage is illustrated in Fig. 13 together with the voltage on the ferroelectric. The current flow in the ferroelectric capacitor is presented in Fig. 14. We observe that like in the experimental data, the current is positive as long as the generator voltage is increasing. As the latter is over its peak value, the current becomes negative. Note the knee in the capacitor voltage. It appears at the same time as the current peak. The maximum value of the current (90 A) is in reasonable accordance with the experiment. In order to understand the details of the functional behavior of the current let us first examine the hysteresis curve in Fig. 15. The large increase in the current occurs in the first 50 ns when the voltage is below 600 V (see the knee in Fig. 13). This is about half a way along the lower hysteresis curve. On the other half of this curve the capacitor is still charging but there are clear indications of saturation and as we see in Fig. 14, the charging current is dropping until it vanishes as the voltage pulse reaches maximum. From this point on the system follows the upper hysteresis curve. The capacitor discharges at this stage. There is an increasing negative current up to about 270 ns which corresponds to a voltage of about 800 V, which is somewhat less than halfway down the hysteresis curve. In the final stage the discharging current is decreasing and it approaches zero. This latter stage is accompanied, in the experiment, by piezoelectric effects

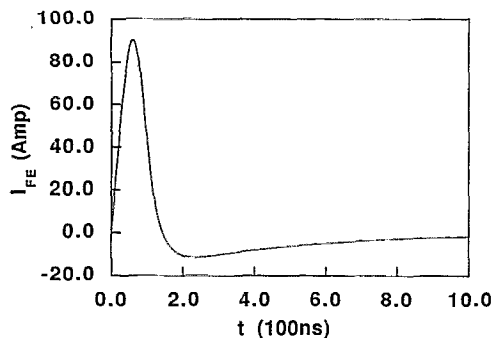


FIG. 14. The current in the ferroelectric capacitor I_{FE} as a function of time.

which have not been considered in the present study and except in this stage the theory is in very good agreement with the experiment.

Now we are in position to examine the entire system, i.e., we consider the grid presence, allow electrons to be repelled into the gap and current to flow in the diode. In the ferroelectric section the only significant difference is that part ($1/\pi^3$) of the voltage which we saw previously was on the ferroelectric is now on the grid, so practically the picture remains the same as above. In the diode mesh, the transmission line is charged to 400 V and its length corresponds to a 500 ns pulse. The resistance induced by the ferroelectric in the gap is illustrated in Fig. 16 assuming that $\nu=0.5$. The corresponding anode current is illustrated in Fig. 17; at 400 ns the current is about 11 A.

The amount of charge in the gap may affect significantly the current at the early stages of the pulse as indicated in Figs. 18 and 19 where the anode current and the gap resistance are calculated assuming that all the ferroelectric charge is in the gap, i.e., $\nu=1$. In Fig. 20 the anode voltage is plotted together with the grid voltage. We observe that after the first quarter of the pulse duration there is a very good correlation between the two voltages.

Finally the case that no voltage was applied on the transmission line ($V_{TL}=0$) has been investigated. In this case we chose $g=2$ mm and again we assume that half of the ferroelectric electrons are in the gap ($\nu=0.5$). The

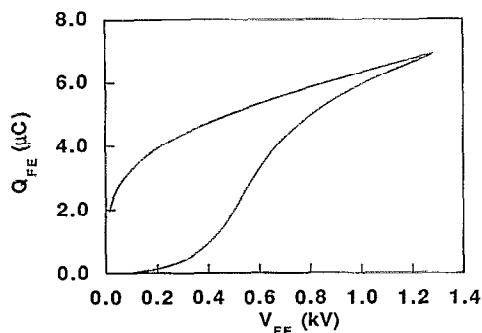


FIG. 15. The hysteresis curve followed by the ceramic during the pulse.

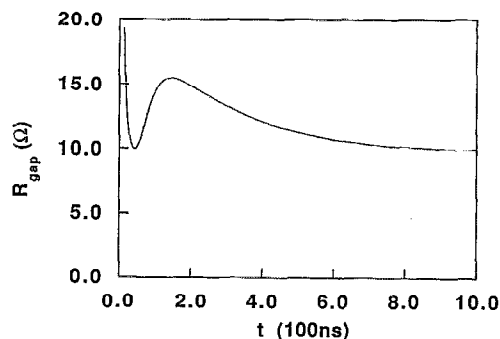


FIG. 16. The resistance induced by the ferroelectric in the gap as a function of time. Half of the ferroelectric electrons are assumed to be in the gap.

resistance in this case appears to be very low (see Fig. 21) and the maximum current (Fig. 22) is about 1.5 A.

IV. DISCUSSION AND CONCLUSIONS

In this study we have examined the operation of a diode with a ferroelectric cathode. The voltage applied on the back of the ferroelectric is entirely responsible for the emission process. From this perspective the device is similar to thermionic emission or photoemission devices in the sense that it is not the diode voltage which is actually extracting the electrons from the material. However, this is a controlled field emission device since the electrons are extracted from the material by an electric field applied on the back of the ferroelectric.

The role of the cathode geometry in this device is far more important than in regular field emission devices. The gridded electrode permits the coupling between the ferroelectric region and the diode gap. Without this coupling the system would operate like a regular field emission diode and for the parameters of interest practically no current would flow. The special geometry of the electrode permits the "penetration" of the potentials space harmonics from the ferroelectric region into the gap. This local field can be very high and it can easily extract electrons from the metallic grid.

The electrons extracted from the metallic grid are not free electrons; they are neutralized by the same amount of

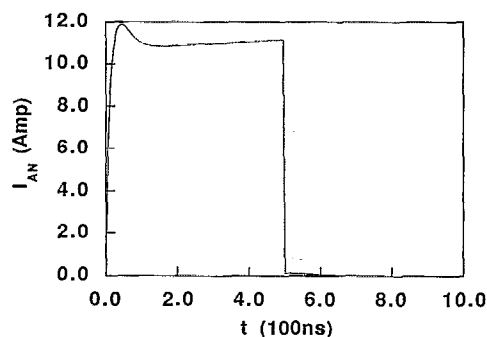


FIG. 17. The anode current as a function of time.

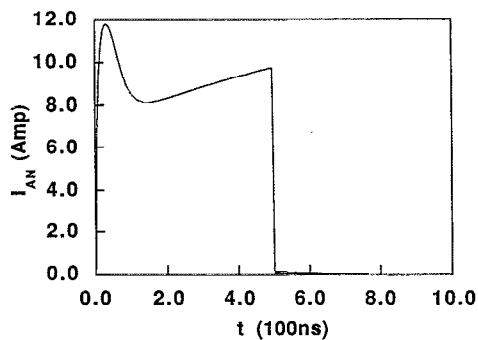


FIG. 18. The anode current as a function of time; in this case all the electrons from the ferroelectrics surface are in the gap.

positive charge on the back electrode; These electrons form a cloud in the gap. The electrons in the gap and the boundary conditions associated with the gap generate a potential well in which the electrons are oscillating. The net current associated with this motion is zero. However, the average kinetic energy of the electrons in the well can be quite large since it is determined by the change in the electrostatic energy stored in the ferroelectric slab. When the anode voltage is applied it slightly perturbs the electrons motion. But this small perturbation is sufficient to give rise to a significant amount of current. This current is linearly dependent on the anode voltage applied.

For each one of the process we mentioned above we have developed a simplified model: the dynamics of the ferroelectric section is determined by Eqs. (16)–(19). The effect of the grid in the ferroelectric is mainly through its capacitance which was determined in Eq. (28) whereas in the anode circuit the grid acts as a voltage source, see equivalent circuit in Fig. 12. Finally the resistance of the gap was calculated, and the analytical expression for it is brought in Eq. (36). These three models were used to simulate the operation of the entire system and, as shown in the last subsection, the results fit well the experimental data. We conclude this paper with a quantitative comparison of theory and experiment: (1) Experiment: for $g=4$ mm, $V_{TL}=300$ V, $R_{TL}=25$ Ω , and $V_{gen}=1900$ V an aver-

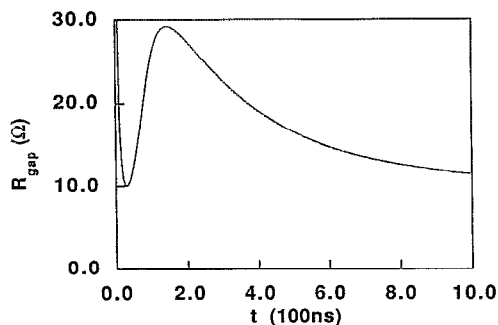


FIG. 19. The resistance induced by the ferroelectric in the gap as a function of time. All the ferroelectrics electrons are assumed to be in the gap.

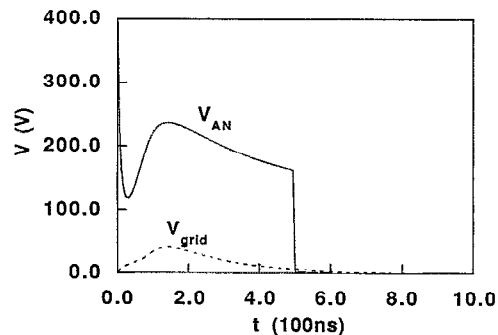


FIG. 20. The variation in time of the anode and the grid voltage.

age current of 8.8 A was measured. (2) Child–Langmuir current for this gap is of order of 30 mA, which is 200 hundred times smaller. (3) The proposed model ($\nu=0.5$) predicts a current which varies along the pulse between 8.4 and 9.0 A in agreement with the experimental data. For another measurement, $V_{TL}=500$ V (the other parameters remain the same), 14 A of current were measured and our theory predicts a current which varies between 13.5 and 14.7 A.

We would like to make some comments now regarding the use of the Child–Langmuir formula in the context of the present device: (1) the only reason is brought here is for those of us who are used to work with field emission diode this gives a common ground for comparison. (2) The voltage applied on the anode in this experiment is not sufficient to extract electrons from either the ferroelectric or the metal (assuming that the former is not pulsed). So basically this is only a “theoretical” comparison. (3) An immediate implication is that since regular field emission does not occur any alternative explanations for the increased current, such as gap closure, are irrelevant to our problem. This does not mean that we rule out the possibility that once the ferroelectric is fired, the anode voltage may cause a variation in space of the cloud distribution. (4) We wish to reemphasize in this context that the current which flows in the diode gap, unlike in regular field emission diodes, cannot be explained without taking into consideration the effect of the ferroelectric and the grid. It

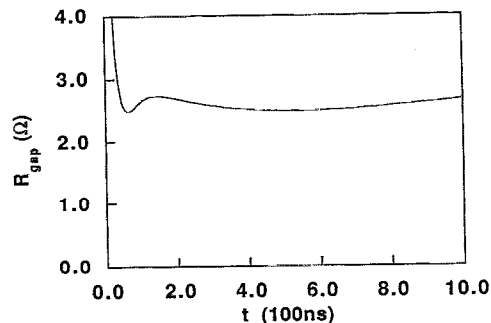


FIG. 21. The resistance induced by the ferroelectric in the gap as a function of time. Half of the ferroelectrics electrons are assumed to be in the gap. The gap is 2 mm wide and $V_{TL}=0$.

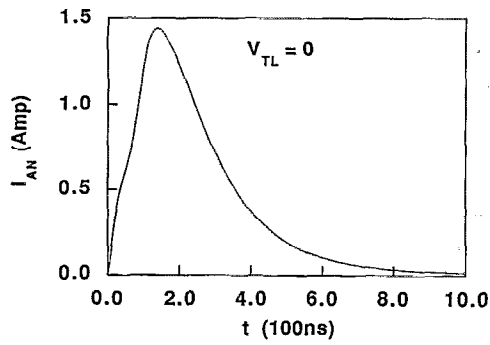


FIG. 22. The variation in time of the anode current when no voltage is applied on the transmission line $V_{TL}=0$. The gap is 2 mm wide. Half of the ferroelectrics electrons are assumed to be in the gap.

is the *strong electrostatic coupling* which allows the increased amount of current. (5) It is the same coupling which induces the deep potential well in the gap [see Eq. (36) and discussion thereafter] as indicated by the gap resistance. These effects have no equivalent in regular field emission devices.

Since the emission is controlled by an external field, this device can be used in low voltage microwave devices where regular field emission is not possible and thermionic emission or photoemission are not desired because of beam quality constraints. In fact even in case when regular field emission is possible but the constraints on the beam quality are very stringent, this kind of emission may be advantageous since it enables extraction at *low* voltage. And it is well known that the emittance of beams for free-electron lasers or accelerators is determined at the early stages of emission in the region where the velocity is still low.

ACKNOWLEDGMENT

This work was supported by the United States Department of Energy.

APPENDIX A: ELECTRIC PARAMETERS

The model for the constitutive relation for the ferroelectric material suggested in Eq. (1) is an approximation of an exact solution of the polarization dynamics as determined in Eq. (9). The relation between the parameters of the model (i.e., E_0 , P_0 , and ϵ) and the parameters of the equation (E_1 , P_1 , and ϵ_r) is given by

$$P_1 = \epsilon_0 E_0, \quad (A1)$$

$$E_1 = \frac{E_0}{\epsilon - 1}, \quad (A2)$$

$$\epsilon_r = (\epsilon - 1) \frac{P_0}{\epsilon_0 E_0} \tanh^{-1} \left(\frac{P_0}{\epsilon_0 E_0} \right). \quad (A3)$$

According to the best fit of the experimental data this implies that $E_1 \approx 0.55$ MV/m, $P_1 \approx 1.47 \times 10^{-2}$ C/m², and $\epsilon_r \approx 2180$.

APPENDIX B: THE DISTRIBUTION OF THE ELECTRONS NEAR THE CATHODE

The charge which screens the polarization field of the material must have a spatial distribution which depends on the electrical characteristics of the material and its geometry. Furthermore, this charge distribution is expected to vary when the polarization field is changed. In this Appendix we shall address these issues. For this purpose a simplified model of our system: consider a dielectric (ϵ_{FE}) slab of a thickness d which has on its rear surface ($z = -d$) a metallic electrode which is grounded. This dielectric models the ferroelectric. In the front surface of the system there is a spatial distribution of electrons $\rho(x, z)$.

Since later we shall want to introduce the effect of the grid, we can write the solution of the Poisson equation in the following form: in the dielectric

$$\phi(x, z) = \sum_n A_n \sinh(|k_n|(z+d)) e^{-jk_n x}, \quad (B1)$$

and the cloud region

$$\phi(x, z) = \sum_n B_n e^{-q_n z} e^{-jk_n x}. \quad (B2)$$

In these equations $k = 2\pi n/L$ where L is the periodicity. Note that in this notation the charge density of the cloud is given by

$$\rho(x, z) = -\epsilon_0 \sum_n B_n (q_n^2 - k_n^2) e^{-q_n z} e^{-jk_n x}. \quad (B3)$$

The decay parameters of the various harmonics in the cloud (q_n) are also the "eigenvalues" of this system which are determined by imposing the boundary conditions at $z=0$. The result is

$$\frac{d \tanh(k_n d)}{\epsilon_{FE} k_n d} = \frac{1}{q_n}. \quad (B4)$$

This equation can be solved for q_n . The solution which is most relevant to our problem is the case when $n=0$ and thus

$$q_0 = \frac{\epsilon_{FE}}{d}. \quad (B5)$$

If we take as a typical value for the dielectric which we show it can be as high as $\epsilon_{FE} = 3000$, then we observe that the whole bunch of electrons is concentrated in a region which for a $d = 1$ mm sample is less than $1 \mu\text{m}$ thick. But in the same time the expression in Eq. (B5) indicates that if in the process of pulsing the ferroelectric the effective dielectric coefficient decreases to $\epsilon_{FE} = 1$, then the cloud "expands" into the gap region for several mm's. An additional feature which is revealed by the last expression is the dependence of the cloud distribution on the ferroelectric thickness. As the sample is getting thicker, more electrons are required to screen the polarization field and thus the electron cloud is getting thicker (q_0 gets smaller).

The presence of the grid can be now included into our calculations by assuming that the potential is zero on the

grid and some effective value $2V_g$ in between. This determines the amplitudes A_n and B_n ; the latter reads

$$B_n = 2V_g \frac{1}{jk_n L} [e^{jk_n L/2} - 1]. \quad (\text{B6})$$

Here it was assumed that the metallic strip occupies half of the period. It is straightforward now to determine the total amount of charge by integrating the expression in Eq. (B3). The result is

$$Q = -A\epsilon_0\epsilon_{\text{FE}} \frac{1}{d} V_g, \quad (\text{B7})$$

where as before A is the diode area. Note that in order to sustain $10 \mu\text{C}$ near the surface the gap average voltage has to be of -12 MV for $\epsilon_{\text{FE}} = 1$. Here we have demonstrated what was mentioned in the text, namely, that the presence of the screening charge generates a deep potential dipression near the surface.

Finally it is interesting to examine the role of the anode in these processes. If we place another grounded electrode at $z=g$, Eq. (B4) takes the following form:

$$\frac{d}{\epsilon_{\text{FE}}} \frac{\tanh(k_n d)}{k_n d} = \frac{\tanh(q_n g)}{q_n}. \quad (\text{B8})$$

If g is significantly larger than L , the gap has no effect on the high order q_n . Regarding q_0 the situation is different: if

ϵ_{FE} has a high value again the gap has no influence but, if $\epsilon_{\text{FE}} \approx 1$ then the gap may have a dramatic effect. For example, if $g < d$ and $\epsilon_{\text{FE}} = 1$ then the possible solutions of Eq. (B8) are (a) $q_0 = 0$, which means that electrons are uniformly filling the gap or (b) that no electrons can be made available to screen the ferroelectric and therefore they all will concentrate on the anode. In both cases the variation in time of ϵ_{FE} causes a significant current flow in the anode although it is grounded, and this was not observed experimentally.

¹H. Riege, CERN-PS 89/42 (AR) 1989.

²H. Gundel, H. Riege, E. J. N. Wilson, J. Handerek, and K. Zioutas, Nucl. Instrum. Methods Phys. Res. A **280**, 1 (1989).

³H. Riege, CERN-PS-NOTE 89-15 (AR) 1989.

⁴A. S. Airapetov, G. A. Gevorgian, I. I. Ivanchik, A. N. Lebedev, I. V. Levshin, N. A. Tikhomirova, and A. L. Feoktistov, Particles Acceleration Meeting.

⁵J. A. Nation, J. D. Ivers, G. S. Kerslick, and L. Schachter, IEEE Particles Accelerator Meeting, San Francisco, May 1991.

⁶J. D. Ivers, L. Schachter, J. A. Nation, and G. S. Kerslick, Bull. Am. Phys. Soc. **36**, 2379, October (1991).

⁷J. D. Ivers, G. S. Kerslick, J. A. Nation, and L. Schachter, Proceedings of Beams '92, Washington, D.C., April 1992.

⁸L. Schachter, J. D. Ivers, J. A. Nation, and G. S. Kerslick, Proceedings of the Workshop on Advanced Acceleration Concepts, June 1992.

⁹J. D. Ivers, L. Schachter, J. A. Nation, G. S. Kerslick, and R. Advani, J. Appl. Phys. **73**, 2667 (1993).

¹⁰*An Introduction to the Physics of Ferro-electrics*, Mitsui Toshio (Gordon & Breach, New York, 1976).